

STABILITY OF RADIATIVE RELATIVISTIC SHOCKS TO GLOBAL OSCILLATIONS

A. KÖNIGL

*Department of Astronomy & Astrophysics,
University of Chicago, Chicago, IL 60637, USA
arieh@jets.uchicago.edu*

J. GRANOT

*Centre for Astrophysics Research, University of Hertfordshire,
Hatfield AL10 9AB, UK
j.granot@herts.ac.uk*

Received 1 February 2008
Accepted 22 February 2008

Thermally emitting, radiative, Newtonian shocks exhibit a global oscillatory instability. The luminosity variations that accompany such oscillations raise the possibility that, if relativistic shocks that emit nonthermal (synchrotron and inverse-Compton) radiation are also subject to such an instability, this could be relevant to the interpretation of certain flares observed in relativistic jet sources associated with AGNs and GRBs. A linear stability analysis, using the equations of special-relativistic MHD and accounting for both the energy and the momentum carried by the radiation, has, however, revealed no unstable modes for physically plausible parameter values. The likely explanation is that, even though synchrotron cooling gives rise to a local radiative instability, the dependence on the magnetic field amplitude is not strong enough to counter the stabilizing effect of enhanced magnetic pressure, due to cooling-induced compression, on the global behavior of the shock. Numerical simulations are under way to ascertain that this conclusion continues to hold also in the nonlinear regime.

Keywords: Relativistic shocks; radiative instability; magnetohydrodynamics; active galactic nuclei; gamma-ray bursts.

1. Introduction

The concept of a *radiative instability*^a has played an important role in astrophysics for over five decades now.¹ It was originally considered in the context of the Sun, the interstellar medium (ISM), and galaxy formation. It was reasoned that, if a diffuse gas is in thermal equilibrium as a result of temperature-independent heating and temperature-dependent radiative cooling, then, if near equilibrium the radiative

^aThe equivalent designation as a *thermal* instability is avoided here to prevent confusion, since the radiation processes under consideration are purely *nonthermal*.

losses increase with decreasing temperature, a perturbation would lead to a thermal runaway in which a cooler-than-average region would cool more effectively than its surroundings. The instability is likely to proceed at constant pressure, so the instability criterion for a perfect gas is²

$$\left(\frac{\partial \mathcal{L}}{\partial T}\right)_p = \left(\frac{\partial \mathcal{L}}{\partial T}\right)_n - \frac{n_0}{T_0} \left(\frac{\partial \mathcal{L}}{\partial n}\right)_T < 0, \quad (1)$$

where \mathcal{L} is the cooling rate per unit volume, p , n , and T are the pressure, number density, and temperature, respectively, and the subscript “0” denotes the equilibrium state. For a diffuse gas one typically has $\mathcal{L} \propto n^2 \Lambda(T)$, with $\Lambda(T) \propto T^\alpha$, in which case instability occurs for $\alpha < 2$. Numerical simulations have verified that the nonlinear evolution of this instability leads to the formation of condensations (often termed “clouds” or “knots”), which in the presence of an ordered magnetic field take the shape of filaments.

The phenomenon described in the preceding paragraph represents a *local* instability. However, about 30 years after it was first identified, numerical simulations of accretion onto a stellar surface³ indicated that the instability can also have a *global* realization in radiative shocks where the postshock fluid is in the unstable regime of the cooling curve $\Lambda(T)$.^b Nearly planar radiative shocks often lead to the formation of a *cold dense layer* of accumulated shocked gas at the end of the postshock cooling zone, which has motivated the common formulation of the problem in terms of a *shock standing off a wall* even in cases that do not involve accretion (see Fig. 1). This layer acts effectively as a “piston head,” and the standoff distance of the shock front from it is of the order of the size of the cooling zone, $x_s \sim v_{\text{ps}} (e/\mathcal{L})$ (where v_{ps} is the velocity of the postshock flow and e is the internal energy density).

The physical origin of the global radiative instability can be understood by considering a perturbation of the shock (or, equivalently, “piston”) speed. If the perturbation is to a larger (resp., smaller) value, the postshock temperature will become correspondingly higher (resp., lower), which in the unstable cooling regime will lead to weaker (resp., stronger) cooling, requiring a longer (resp., shorter) cooling length and hence a further increase (resp., decrease) in the shock speed. In the nonlinear regime this instability results in global oscillations of the shock front with respect to the cold dense layer on a time scale $\sim t_{\text{cool}}$, which in extreme cases can involve the complete collapse of the cooling region (“catastrophic” cooling⁴). The proposed astrophysical applications of this mechanism in the case of thermally emitting Newtonian shocks have included accretion flows onto compact objects, supernova remnants, interstellar (wind) bubbles, colliding winds, and Herbig-Haro objects (the heads of jets from newly born stars).

^bA shock is radiative if the following two conditions are met: (1) it is in the fast-cooling regime, i.e. the cooling time t_{cool} of the radiating component (which in relativistic shocks is typically electrons and positrons) is shorter than the dynamical time $t_{\text{dynamical}}$ of the shock, and (2) the radiating component contains most, if not all, of the thermal energy behind the shock (or, equivalently, the parameter ϵ_e defined below is not $\ll 1$).

This contribution considers the possibility that a global radiative instability applies also to nonthermally emitting relativistic shocks. Such shocks evidently occur in relativistic jet sources, particularly those associated with active galactic nuclei (AGNs) and gamma-ray bursts (GRBs). These sources exhibit variable non-thermal emission that is often characterized as “flares.” Some of the observed flares show a pronounced oscillatory behavior, and in certain cases it can be argued that the associated shocks are radiative. Such shocks would be prime candidates for this mechanism if indeed it could be shown to operate in these systems.

Previous work on thermally emitting Newtonian shocks (including the effect of a transverse magnetic field) and on local radiative instability of a nonthermally emitting gas is summarized in Secs. 2 and 3, respectively. Section 4 presents and explains the results of a linear stability analysis, which indicate that nonthermal relativistic shocks are not susceptible to a global instability of this type, and describes a numerical scheme that is being utilized to simulate such shocks.

2. Global Instability of Thermal Newtonian Shocks

The linear stability analysis for this case was first performed by Chevalier and Ima-mura,⁵ who considered a plane-parallel shock with $\mathcal{L} \propto n^2 T^\alpha$ and stationary-wall boundary conditions. They found that the shock is *overstable* (i.e. the shock-front position oscillates with exponentially growing amplitude) in the *fundamental mode* for $\alpha \lesssim 0.4$ and in the first and second *overtone modes* for $\alpha \lesssim 0.8$, with an oscillation frequency $0.3 (v_s/x_{s0})$ for the fundamental mode and $0.6 - 1.0 (v_s/x_{s0})$ for the first overtone mode for α between -1 and 2 (where v_s is the upstream fluid velocity with respect to the wall). It was subsequently demonstrated that the results are not qualitatively modified when more realistic cooling functions and unequal electron and ion temperatures are taken into account, or when different downstream boundary conditions are employed. The inclusion of transverse perturbations (i.e. perpendicular to the shock normal) does not introduce new modes, but it destabilizes the parallel fundamental and first-overtone modes already for $\alpha \lesssim 1.0$.⁶ The linear analysis also indicated that transverse perturbations could modify the luminosity behavior of the shock.⁷

The nonlinear evolution of the instability has been investigated numerically by various groups. For example, Walder and Folini⁸ carried out 1D simulations and found a variety of behaviors, ranging from smooth, sinusoidal oscillations in shock position and integrated luminosity with $\mathcal{O}(1)$ amplitudes to abrupt, large-amplitude (up to 2 orders of magnitude) variations associated with catastrophic cooling and accompanied by the formation of secondary shocks. The manifested behavior is evidently determined by the form of the cooling curve $\Lambda(T)$ that corresponds to the postshock temperature of the stationary shock solution. Mignone⁹ also performed 1D simulations and found that the saturated oscillatory phase is characterized by a “main sequence” of overtones but that these modes also exhibit complex nonlinear interactions. Sutherland *et al.*¹⁰ did both 1D and 2D simulations and found evidence

that the amplitudes of the second and subsequent shock bounces in the 2D case are reduced by a factor of ~ 2 compared to the 1D results, likely because more dynamical modes are available to siphon away the shock kinetic energy.

The presence of a transverse magnetic field of amplitude B has a purely *stabilizing* influence on thermal shocks. In this case $B \propto n$, so, as cooling increases the compression and n goes up, so does also the magnetic pressure $B^2/8\pi$, which resists further compression and provides a “cushioning” effect that opposes the shock-front collapse. The strength of the magnetic field is parameterized in the Newtonian limit by the *Alfvén Mach number* $M_A = v_s/v_A$, where v_A is the upstream Alfvén speed. Linear and nonlinear calculations^{11–13} have determined that all modes can be stabilized by a comparatively weak field ($M_A < 8$) when $\alpha > 0$ and by an even weaker field ($M_A < 33$) when $\alpha > 0.5$, but that a typical interstellar field may not be strong enough to stabilize a sufficiently fast shock that produces a negative postshock value of α .

3. Local Instability of Nonthermally Emitting Gas

The *Newtonian* system of equations for a gas composed of nonrelativistic protons (which dominate the inertia) and relativistic electrons (with a Maxwellian or a power-law energy distribution) that emit synchrotron and inverse-Compton radiation was linearized by a number of authors.^{14–16} The parameters of the problem are the *magnetic-to-thermal* and the *photon-to-magnetic* energy density ratios, which measure, respectively, the dynamical importance of the magnetic field and the relative contribution of the synchrotron and inverse-Compton radiation processes. It was found that synchrotron-emitting gas can become unstable to perturbations with wavevectors that are perpendicular to the magnetic field if the magnetic-to-thermal pressure ratio is $< 1/4$ and that inverse-Compton losses (for a given external radiation field) are stabilizing. The instability condition is again the isobaric criterion given by the analog of Eq. (1), but with p replaced by the total pressure $p + B^2/8\pi$.

The physical basis of the instability can be understood from the dependence of the synchrotron emissivity on the magnetic field amplitude.¹⁷ For the case of a monoenergetic relativistic electron distribution with a (random) Lorentz factor γ_e and number density n_e , $\mathcal{L}_{\text{synch}}$ is given by

$$\mathcal{L}_{\text{synch}} = \frac{c\sigma_T}{6\pi} \gamma_e^2 n_e B^2, \quad (2)$$

where c is the speed of light and σ_T is the Thomson cross section. Under ideal MHD conditions, the magnetic field amplitude increases with density. Thus, a perturbation that increases B enhances the cooling, which in turn induces compression that further increases B .

Numerical studies of the nonlinear evolution of the instability have verified that it could potentially account for the formation of bright knots and filaments in pulsar-wind nebulae and in extragalactic radio sources.^{18,19}

4. Global Stability of Nonthermal Relativistic Shocks

The occurrence of a local radiative instability in a synchrotron-emitting gas raises the possibility that, as in the thermal emission case, a shock cooling by nonthermal radiation might be subject to a global oscillatory instability. On the other hand, the “cushioning” effect of a transverse magnetic field, which was found to stabilize purely thermal shocks, should apply (and, in fact, be inherently present) in this case as well. Furthermore, although inverse-Compton cooling by an external radiation field was shown to have a purely stabilizing influence on a local instability, it might have a more complex influence on a global instability of a hydromagnetic shock in that it would increase (through induced compression and resultant field amplification) the relative contribution of synchrotron radiation cooling as the shocked gas moved downstream in the cooling zone.^c The outcome of these potentially competing effects, which determines whether a global instability indeed exists in this case and the range of its properties if it does, must be investigated by explicit calculations. Since the astrophysical circumstances under which this instability might arise likely involve relativistic motions, a fully covariant special-relativistic treatment that allows for large bulk and random Lorentz factors is required in this study.

4.1. Linear stability analysis

This analysis has been carried out by Granot and Königl, and full details are given in Ref. 21. It is patterned after the Newtonian treatment of thermally emitting shocks in Ref. 5 but specializes to the ultrarelativistic limit (preshock bulk Lorentz factor and postshock random Lorentz factors $\gg 1$), which leads to a distinct formulation that cannot be simply reduced to the Newtonian case.

4.1.1. Formulation

The setup is as shown in Fig. 1: a planar shock is located at a distance x_s from a “wall” (or “piston”) that is fixed at $x = 0$. The position of the perturbed shock oscillates about x_{s0} , the equilibrium shock–piston separation, which is assumed not to vary on the time scale of the oscillations. All velocities are measured in the rest-frame of the piston. In this frame, the *ambient* gas (subscript “a”) flows in with a 4-speed $u_a \gg 1$. The shock is assumed to be *strong*, with effectively infinite thermal and Alfvén Mach numbers. In this case the fluid 4-velocity $u_2 = \gamma_2 \beta_2$ immediately behind the shock transition (subscript “2”) can be expressed as a function only of the magnetization parameter σ_a (defined below), independent of the shock speed. The gas is composed of protons and neutralizing electrons and/or electron-positron pairs (parameterized by $\chi \equiv n_{e^+}/n_{e^-}$). Both the proton and the e^\pm components are

^cBoth of these effects, which arise from cooling-induced postshock field amplification, were explicitly demonstrated in the nonthermal hydromagnetic shock models of Granot and Königl.²⁰

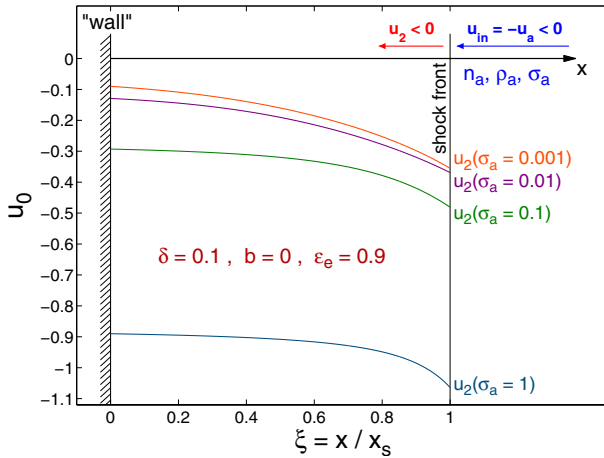


Fig. 1. Sketch of a radiative relativistic shock standing off a “wall.” The equilibrium 4-velocity profiles for several combinations of the model parameters are superposed. The notation and further details are given in the text.

taken to have an *ultrarelativistic equation of state* behind the shock ($w = 4p$, where w is the enthalpy density). The upstream gas is assumed to be cold ($w_a \approx \rho_a c^2$, where ρ is the rest-mass density).

The shock is assumed to be transversely magnetized and to obey ideal MHD. In this case one can show that $\mathbf{B}/n = \text{const}$ in both the steady and the perturbed flow. The field strength is determined by the upstream magnetization parameter $\sigma_a \equiv u_{Aa}^2$, where $u_{Aa}^2 = B_a^2/4\pi w_a \approx B_a^2/4\pi\rho_a c^2$ is the square of the upstream Alfvén 4-velocity. An alternative parameterization is in terms of ϵ_B , the magnetic-to-internal energy ratio immediately behind the shock transition, which can be expressed as a function of σ_a .

The shock emission is assumed to be purely nonthermal and to involve *synchrotron radiation* and *inverse-Compton scattering* of the synchrotron photons (SSC) and possibly also of an external radiation field (ERC) by locally monoenergetic electrons and positrons. (The protons are assumed to evolve adiabatically with an adiabatic index of $4/3$.) Thus, $\mathcal{L} = (1+Y)\mathcal{L}_{\text{synch}}$, where $\mathcal{L}_{\text{synch}}$ is given by Eq. (2) and Y is the Compton- y parameter. The energy available for radiation is determined by the parameter ϵ_e , the fraction of the internal energy in e^\pm immediately behind the shock transition, and the relative contribution of the inverse-Compton process is fixed by Y_2 , the value of Y at that location. One can write

$$Y_2 = b + \frac{(1+b)}{2} \left(\sqrt{1 + \frac{4a}{(1+b)^2}} - 1 \right) \tag{3}$$

(see Ref. 20), where $a \equiv k_2 u_2^2 (\beta_2^{-1} - 1) \epsilon_e / \epsilon_B$ (with k_2 being a numerical coefficient $\mathcal{O}(1)$) and $b \equiv e_{\text{ph}2}^{\text{ext}} / e_{B2}$ (the ratio of the external-photon and the magnetic energy

densities behind the shock transition). Equation (3) (with $k_2 \approx 1$) demonstrates that the SSC radiation component is determined directly by the parameters ϵ_e and ϵ_B . Hence Y_2 can effectively be replaced by the parameter b that measures the relative strength of the external radiation field (which, when present, is taken to be isotropic in the upstream rest frame).

The particle density n , rest-mass density ρ , magnetic field amplitude B , as well as w , p , and \mathcal{L} are measured in the *local rest frame of the fluid*. The shock is analyzed using the covariant conservation equations for particle number, momentum, and energy:

$$\frac{\partial}{\partial t}(\gamma n) + c \frac{\partial}{\partial x}(\gamma \beta n) = 0, \quad (4)$$

$$\frac{\partial}{\partial t}(\gamma^2 \beta w_{\text{tot}}) + c \frac{\partial}{\partial x}(\gamma^2 \beta^2 w_{\text{tot}} + p_{\text{tot}}) = -\gamma \beta \mathcal{L}, \quad (5)$$

$$\frac{\partial}{\partial t}(\gamma^2 w_{\text{tot}} - p_{\text{tot}}) + c \frac{\partial}{\partial x}(\gamma^2 \beta w_{\text{tot}}) = -\gamma \mathcal{L}, \quad (6)$$

where $w_{\text{tot}} \equiv w + (B^2/4\pi)$ and $p_{\text{tot}} \equiv p + (B^2/8\pi)$. The appearance of radiative cooling terms of comparable magnitudes on the right-hand sides of Eqs. (5) and (6) indicates that, in contrast with the Newtonian case, both the energy *and* the momentum of the emitted radiation can play an important role in highly relativistic shocks.

The shock equations have been linearized (setting $u(\xi, t) = u_0(\xi) + u_1(\xi)e^{\omega t}$, etc., where $\xi \equiv x/x_s$) with respect to the equilibrium solution derived in Ref. 20. In this solution, the “wall” is identified with the location where the internal energy of the e^\pm component completely vanishes, which formally only occurs asymptotically. This requires the introduction of another numerical parameter ($\delta \ll 1$) that allows an effective postshock cooling distance x_{s0} to be defined. Altogether, the parameters of the problem are thus ϵ_e , σ_a (or ϵ_B), Y_2 (or b), and δ . (The composition parameter χ is not included in this list since it only affects the value of the equilibrium cooling length x_{s0} and hence just the normalization of x .)

Several equilibrium velocity curves, corresponding to different values of σ_a (with the other parameters held fixed) are plotted in Fig. 1.

One obtains six ODEs for the real and imaginary parts of the dimensionless perturbations of the velocity (η), pressure (Π), and number density (ζ), and uses the boundary conditions at $\xi = 0^d$ to determine (iteratively) the dimensionless complex frequency $\psi = \psi_R + i\psi_I$ as the eigenvalue of the problem (with $\psi_R > 0$, $|\psi_I| > 0$ and $\psi_R < 0$, $|\psi_I| > 0$ indicating an overstability and decaying oscillations, respectively).

^dSo far only the standard “wall” BC $u_1(\xi = 0) = 0$ has been considered.

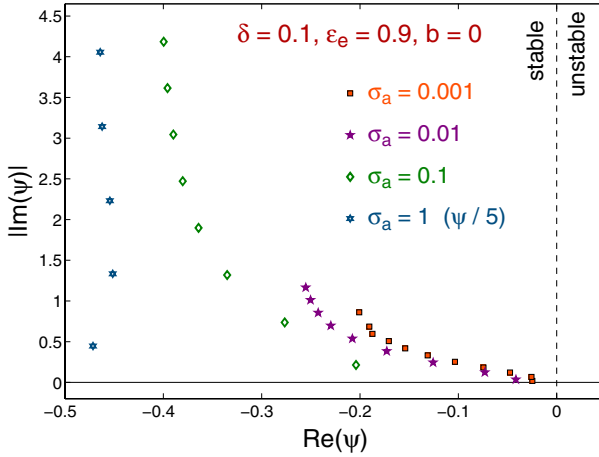


Fig. 2. Normalized complex frequencies of the global modes obtained by linearizing about the equilibrium shock solutions shown in Fig. 1.

4.1.2. *Results*

Although the investigation is not yet complete and only a limited number of parameter combinations have been examined, the indications so far are that the model shock under consideration is *linearly stable* to global oscillations. Figure 2 shows the derived eigenvalues in the complex frequency plane for the equilibrium solutions exhibited in Fig. 1. The successive modes for each 4-parameter combination are clearly seen, and all are located in the stable region to the left of the $\psi_R = 0$ line.

These results are not entirely surprising. If the magnetization parameter σ_a is $\ll 1$ then the pressure immediately behind the shock is thermally dominated.^e For the adopted monoenergetic particle distribution the constant pressure constraint then implies $n_e \propto 1/\gamma_e$. Using also $B \propto n_e$, one infers from Eq. (2) that $\mathcal{L}_{\text{synch}} \propto 1/\gamma_e$.^f Treating γ_e as the temperature T in the expression $\mathcal{L} \propto T^{\alpha-2}$ considered in Sec. 1, we infer that, heuristically, the synchrotron emission case corresponds to an effective temperature power-law index $\alpha = 1$. As summarized in Sec. 2, for this value of α a thermal Newtonian shock is already stable to global oscillations in the fundamental and first overtone modes even before any magnetic field effects further stabilize it. When a magnetic field is present, all modes are stabilized for $M_A^{-2} \gtrsim 9 \times 10^{-4}$ when $\alpha > 0.5$, and for an even smaller (in fact, much smaller) value of M_A^{-2} when α increases to 1 (see Fig. 3 in Ref. 11 and Fig. 4 in Ref. 13).

^eIndeed, in this case the postshock magnetic and thermal pressures are $\sim 8(B_a^2 u_a^2 / 8\pi)$ and $\sim (2/3)\rho_a u_a^2 c^2$, respectively, so the ratio between them is $\sim \sigma_a$.

^fUnder similar assumptions, one infers $\mathcal{L} \propto \gamma_e^0$ and $\propto \gamma_e$ when the SSC and ERC components, respectively, dominate, indicating neutral and stabilizing local responses, respectively, to enhanced cooling.

The relativistic analog of M_A^{-2} is σ_a (which, as noted above, similarly fixes the postshock magnetic-to-thermal pressure ratio). This correspondence indicates that it is indeed plausible that all modes shown in Fig. 2 remain stable even for the lowest plotted value (10^{-3}) of σ_a .

Values of σ_a much smaller than $\sim 10^{-3}$ are not often inferred in the relativistic astrophysical shocks (such as the GRB afterglow shocks^{22,23}) to which this mechanism could potentially apply. Furthermore, in the limit when σ_a (or, equivalently, ϵ_B) is $\ll 1$ but ϵ_e remains ~ 1 (as required for efficient cooling), the postshock Compton- y parameter is $Y_2 \approx (\epsilon_e/\epsilon_B)^{1/2} \gg 1$ (see Eq. (3)), implying that the SSC radiation component, rather than the synchrotron component that drives the instability, dominates the emission. It thus appears that, under realistic circumstances, nonthermally emitting relativistic shocks will remain linearly stable to global oscillations. Given, however, the finding in the thermal Newtonian case that the various modes exhibit complex interactions in the nonlinear regime,⁹ it is of interest to check the above conclusion with numerical simulations. The numerical scheme that is being utilized for this purpose is described in the following subsection.

4.2. Numerical simulations

This study is carried out in collaboration with A. Mignone. The relativistic MHD (RMHD) equations are solved using the PLUTO code.²⁴ PLUTO is a modular code offering a multi-physics, multi-algorithm environment specifically oriented toward the treatment of astrophysical flows in the presence of discontinuities. The modular structure exploits a general framework for integrating a system of conservation laws, built on modern Godunov-type shock-capturing schemes. Equations are solved in a conservative way using a finite-volume formulation, whereby volume averages are evolved in time by solving Riemann problems at cell interfaces. Denoting with \mathbf{u}_i^n the vector of conserved variables at time $t = t_n$ in cell i , the integral average $\bar{\mathbf{u}}_i^n$ is advanced in time according to

$$\bar{\mathbf{u}}_i^{n+1} = \bar{\mathbf{u}}_i^n - \frac{\Delta t}{\Delta x} \left(\mathbf{f}_{i+\frac{1}{2}}^{n+\frac{1}{2}} - \mathbf{f}_{i-\frac{1}{2}}^{n+\frac{1}{2}} \right), \quad (7)$$

where fluxes $\mathbf{f}_{i\pm\frac{1}{2}}^{n+\frac{1}{2}}$ are computed as time averages at cell edges. Flux computation requires solving (in an exact or approximate way) a Riemann problem, that is, the decay of an arbitrary discontinuity separating two adjacent states to the left and to the right of a given cell interface.

Second-order accuracy in space is achieved using limited slopes to prevent unwanted spurious numerical oscillations in the vicinity of strong gradients. Predictor-corrector methods can be used to gain second-order accuracy in time.

For the present application, we employ the RMHD module together with the relativistic HLLC Riemann solver developed in Ref. 25 for the case of transversely magnetized flows. The equation of state can be chosen to be either a constant- Γ law ($\Gamma = 4/3$ or $\Gamma = 5/3$ for a hot or a cold gas, respectively) or the approximation to the Sygne gas discussed in Ref. 26.

Source terms are included using operator splitting, that is, by alternately solving the homogeneous set of equations (i.e. without the source term) followed by a source step, where only the effect of the source term is considered.

Work on these simulations has already commenced and the results will be reported elsewhere.

Acknowledgments

We thank A. Mignone for his help in preparing this contribution.

References

1. E. N. Parker, *Astrophys. J.* **117**, 431 (1953).
2. G. B. Field, *Astrophys. J.* **142**, 531 (1965).
3. S. H. Langer *et al.*, *Astrophys. J.* **245**, L23 (1981).
4. S. A. E. G. Falle, *Mon. Not. R. Astron. Soc.* **195**, 1011 (1981).
5. R. A. Chevalier and J. M. Imamura, *Astrophys. J.* **261**, 543 (1982).
6. E. Bertschinger, *Astrophys. J.* **304**, 154 (1986).
7. C. J. Saxton and K. Wu, *Mon. Not. R. Astron. Soc.* **324**, 659 (2001).
8. R. Walder and D. Folini, *Astron. Astrophys.* **315**, 265 (1996).
9. A. Mignone, *Astrophys. J.* **626**, 373 (2005).
10. R. Sutherland *et al.*, *Astrophys. J.* **591**, 238 (2003).
11. G. Tóth and B. T. Draine, *Astrophys. J.* **413**, 176 (1993).
12. P. A. Kimoto and D. F. Chernoff, *Astrophys. J.* **487**, 728 (1997).
13. B. Ramachandran and M. D. Smith, *Mon. Not. R. Astron. Soc.* **362**, 1353 (2005).
14. M. Simon and W. I. Axford, *Astrophys. J.* **150**, 105 (1967).
15. J. A. Eilek and L. J. Caroff, *Astrophys. J.* **233**, 463 (1979).
16. P. Rossi *et al.*, *Astrophys. J.* **414**, 112 (1993).
17. A. P. Marscher, *Astrophys. J.* **239**, 296 (1980).
18. G. Bodo *et al.*, *Astron. Astrophys.* **256**, 689 (1992).
19. E. M. de Gouveia dal Pino and R. Opher, *Mon. Not. R. Astron. Soc.* **263**, 687 (1993).
20. J. Granot and A. Königl, *Astrophys. J.* **560**, 145 (2001).
21. J. Granot and A. Königl, in preparation.
22. T. Piran, *Rev. Mod. Phys.* **76**, 1143 (2005).
23. P. Mészáros, *Rep. Prog. Phys.* **69**, 2259 (2006).
24. A. Mignone *et al.*, *Astrophys. J. Suppl.* **170**, 228 (2007).
25. A. Mignone *et al.*, *Space Sci. Rev.* **121**, 21 (2005).
26. A. Mignone and J. C. McKinney, *Mon. Not. R. Astron. Soc.* **378**, 118 (2007).